ngVLA Memo # 51
Taking a Census of Supermassive Binary Black Holes

Karishma Bansal & Greg Taylor (UNM)

Abstract

In this community study, we take a census of Supermassive Binary Black Holes using the ongoing VLA all sky survey, being conducted at 3 GHz. These candidates are selected such that they are nearby (z< 0.1), bright (i<= 14), and compact. We estimate spectral properties for some of these candidates for which we can obtain a flux density at 1.4 GHz in NVSS. We find that spectral index peaks between -0.5 and -1.0 for our candidates. In order to further confirm these candidates and study their binary orbit, it would require an array of both high sensitivity and resolution. We suggest an array configuration for the upcoming ngVLA such that it satisfies our requirements to undertake this science.

1 Introduction

Supermassive black holes reside at the heart of most major galaxies. They affect the growth and dynamics of their host galaxy. When two such galaxies collide, they are expected to form a supermassive binary black hole (SMBBH) system. Surprisingly, only handful systems have been detected to date (Burke-Spolaor, 2011; Tremblay et al., 2016). This raises various questions such as how often do galaxies collide? Does a collision give rise to a binary system, and how quickly do these black holes merge after binary formation? Understanding these systems is important to understanding fundamental astrophysical problems ranging from galaxy evolution to active galactic nuclei (AGN) to black hole growth.

Additionally, the study of SMBBHs will provide an opportunity to explore how two compact SMBHs interact when in orbit with each other. Analogous to the study of binary stars which helps us estimate their physical properties such as the mass, separation, orientation, and spin, the orbital study of SMBBHs will enable us to determine similar parameters. The SMBBH in 0402+379, with a separation of 7.3 pc between its core components, is one of the few known precursors of GW sources. It has an orbital period estimate of $\sim 30,000$ y (Bansal et al., 2017), which took some 20 y of observation to obtain orbital constraints. Considering that sub-kpc-scale dual AGNs may be relatively rare (as suggested by Comerford et al. (2012)), we need to look at thousands of sources in order to successfully detect a few of them and subsequently, be able to study their orbit.

The orbital period scales with the separation as,

$$P_B = (4\pi^2 a^3/GM_T)^{0.5} = 7500y(\theta_{mas} z_{0.1})^{3/2}/M_9^{0.5}, \quad (1)$$

where M_T is the total mass of the core. The binary SMBH formation takes place when they are at a physical separation of the order of pc (Begelman et al., 1980; Milosavljević & Merritt, 2003), given by $10^6 \frac{c}{H_0}\ \theta\ z$ pc. The further decay of this binary system is driven by different mechanisms, e.g. scattering with individual stars (Begelman et al., 1980) or viscous drag in a circumbinary disc (Cuadra et al., 2009; Roedig et al., 2012). However, the further inspiral is believed to halt at a certain separation due to rapid depletion of stars in the loss cone before gravitational energy loss starts dominating the orbital decay, also known as the last-parsec

problem. Most of the simulations haven't been able to achieve this resolution. Recently, Khan et al. (2011) through their simulations suggest that the hardening rate of binary orbits are higher if we relax the oversimplified assumptions such as symmetric systems. We would like to explore these systems from pc separation to sub-parsec level.

We obtain mass and separation range for two orbital periods, 1000 and 10000 years in Figure 1. The lower limit on the mass is constrained by the luminosity as it scales with the bulge mass, $M_{BH} = 10^9\ M_\odot \sim 0.01 L_\odot$. For the upper limit, we refer to the most massive SMBBH system (21 billion $M_\odot$, McConnell et al. (2011)) in literature. In order to detect SMBBHs systems and obtain their orbital parameters on the order of ~ 10 years, we need massive $\sim 10^7\ M_\odot$ and compact systems with a maximum separation between components ~ 5 pc, at a maximum redshift of 0.1.

These studies are also important to understand jet structures. Bansal et al. (2017) studied the core-shift effect which enabled them to measure the magnetic field near the core. The Very Large Baseline Array (VLBA) has been a very useful instrument to carry out this study, however, it has limited sensitivity. Next generation very large array (ngVLA) with a large number of dishes as well as extended baselines will be the most promising instrument to answer all the above-stated questions.

Our aim is to study more SMBBHs at redshift below 0.1 such that we are close enough to attain the required resolution (sub-pc) for compact binaries such that their orbit can be tracked in about 10 years. Also, we need enough sensitivity to detect low summed black hole mass ($10^7\ M_\odot$). Assuming the above scaling relationship between the bulge mass and luminosity, we can get an estimate of bulge mass. We employ this to estimate brightness cutoff from the Galaxy i band magnitude, a reasonable proxy for bulge luminosity for early-type galaxies.

We use various criteria such as brightness (i <= 14), redshift (< 0.1), and source size ($\sim$ pc) to obtain a census of nearby SMBBH candidates. We mainly select single component sources as the source size is comparable to the beam size. We analyze the quicklook images from the ongoing VLA sky survey (VLASS) to obtain a list of candidates that satisfy all the requirements. This survey surpasses all the previous surveys in terms of sky area and is being conducted at 2 and 4 GHz, close to the turnover frequencies. We also explore possible configurations of ngVLA such that it would be possible to confirm SMBBH candidates and study the orbital dynamics in the future.

2 Source List

2.1 Source Selection

In this study, we take a census of SMBBHs using the ongoing VLASS survey [1]. We take the reduced data from the VLASS, available in the form of quick-look images. We then use PYBDSF (Mohan & Rafferty, 2015), a tool to detect sources in interferometric images and make catalogs with them. This program divides an image into many islands and then fits Gaussians as per the selection cutoff. We have used a cutoff of 7σ for our source selection. Sources are then grouped into three categories: S, M, and C, based on the number of Gaussian components in them, where S denotes single-Gaussian source that is the only source in the island, M denotes multiple Gaussians, and C denotes a single-Gaussian source in an island with other sources. For our purpose, we use only single gaussian compact sources denoted by S.

VLASS has been split into many tiles such that each tile spans 4 degrees in Declination and 360 degrees in RA. Each tile has been further divided into many subsections across RA and Dec. We combine catalogues made from each subsection to make a combined catalogue

[1] https://archive-new.nrao.edu/vlass/

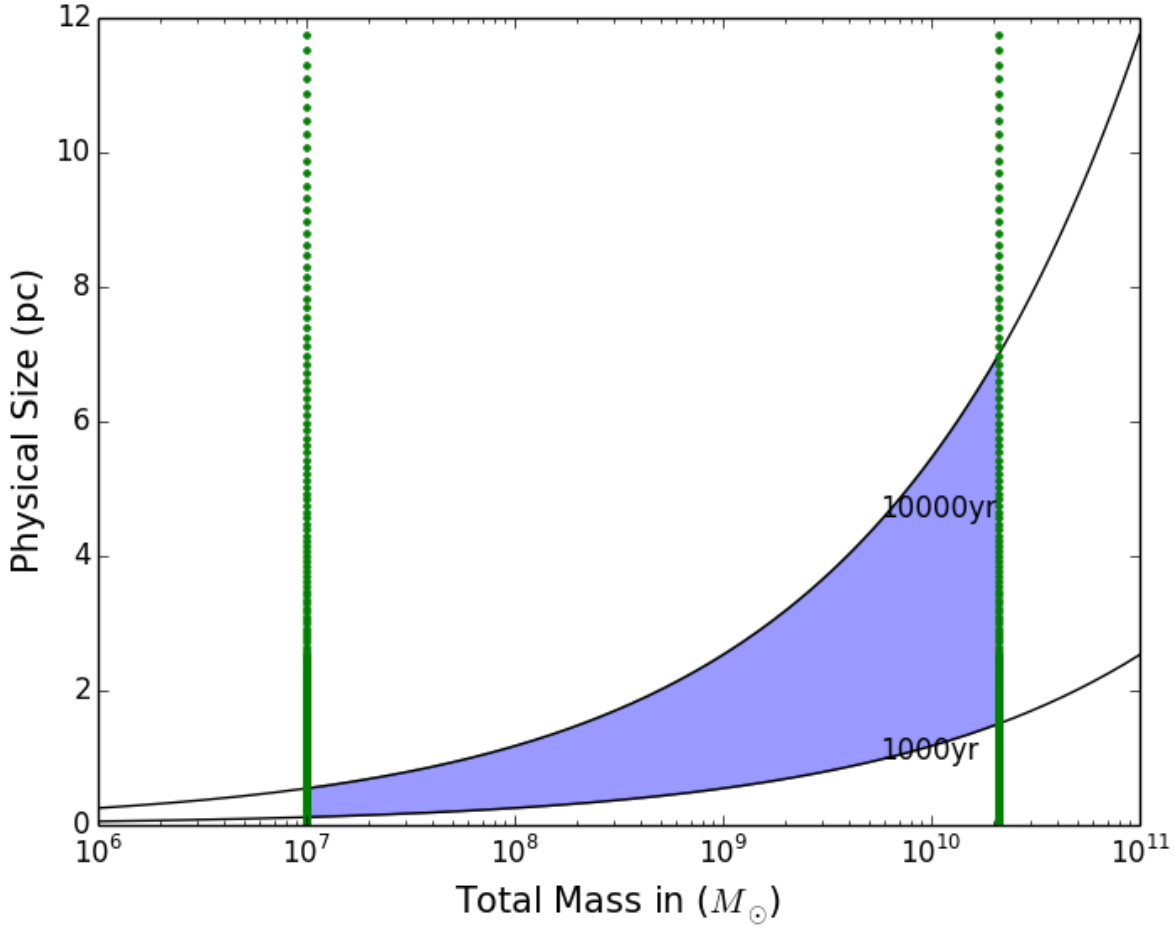

Figure 1: The highlighted region shows our area of interest. It is being bordered by $10^7 M_\odot$ and highest reported SMBBH mass 2.1 $10^{10} M_\odot$ along the x-axis, and physical size estimates at a redshift of 0.1, for orbital period of 1000 and 10000 years in the y-axis.

of one tile. We have used three strips for our source selection. The details of these stripes are listed in Table 1.

Table 1: VLASS Tile Coordinates

Tile	RA (deg)	DEC (deg)
1	0-360	32-36
2	0-360	57-61
3	0-360	61-65

These VLASS catalogues are cross matched with Sloan Digital Sky Survey (SDSS) (Gunn et al., 2006) and NRAO VLA Sky Survey (NVSS) (Condon et al., 1998) catalogues to obtain redshift and spectral index information, respectively.

SDSS is a sky survey which involves optical imaging of the northern sky and spectroscopic measurements in near-infrared, using the 2.5 m Sloan Foundation Telescope at Apache Point Observatory. It is a large survey which contains distances to more than four million galaxies. We have used the recent data release (DR14, Blanton et al. (2017)) for obtaining the catalogues. SDSS sources have been selected such that they are nearby bright galaxies with i-mag <= 14 and redshift< 0.10, and they span the same coordinates as the selected VLASS tiles. Our criterion for cross-matching any two catalogues is the calculated distance between the two sources should be less than ~ 0.0007 degrees (~ 2.5 arcsec). We first cross-match VLASS and SDSS, which gives 221 matches.

Spectral properties help us understand the nature of a source. Flux density dependence on frequency can be defined as $S \propto \nu^{\alpha}$, where α is the spectral index. We expect the radio spectra of low-luminosity accreting black holes to be flat (spectral index ~ 0). In order to obtain a spectral index, we require flux density at two frequencies at the least. VLASS provides flux density at 3 GHz and for the second point, we turn to NVSS, a continuum sky survey conducted at 1.4 GHz north of -40° declination. This contains over 1.8 million discrete sources. The sensitivity of source detection is 0.46 mJy beam^{-1} with a beam width of $45^{'}$. Our selected 221 sources were cross-matched with the NVSS catalog, and we have obtained 50 matches. The reason for this low number is the low sensitivity of the NVSS in comparison to the VLASS which affects the weak source detection. NVSS provides a flux density at 1.4 GHz, using that along with flux density at 3 GHz, we estimate spectral index for these sources. Table 2 contains details of all three surveys.

Table 2: Survey Information

Survey	Beam Size (arcsec)	Frequency/Wavelength	RMS flux
VLASS	2.5	3.0 GHz	0.1 mJy
NVSS	45	1.4 GHz	2.3 mJy
SDSS	8	$380 - 920$ nm	$-$

2.2 Source Statistics

Once we obtain the source catalogue, we study their distribution of flux density and spectral index. Figure 2 shows the flux distribution for 221 sources obtained from cross-matching VLASS and SDSS. All the sources in our selection have flux density < 100 mJy. After cross-matching with NVSS, we find one candidate with flux density higher than 100 mJy at 1.4 GHz. It is a known Seyfert galaxy 1202+6208 at a redshift of 0.00075.

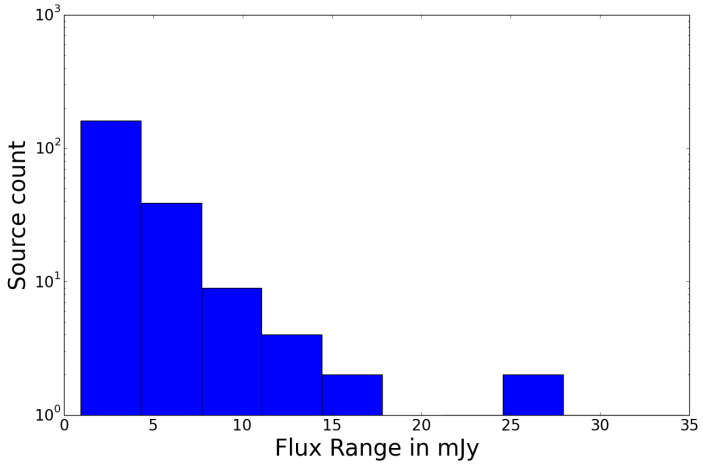

Figure 2: Flux distribution at 3 GHz for 221 sources obtained from cross matching VLASS and SDSS (sec 2.1).

We now estimate the expected number of sources in the entire VLASS, which follow all the above criteria.
Total area covered $= 4 \times (8 \cdot 0.8 + 14 \cdot 1.33 + 16 \cdot 1.33) \times 15 = 2778$ deg^2
Area being surveyed by VLASS = 33885 deg^2 ($> -40°$ in Dec)
Total expected candidates from VLASS $=221 \times 33885/2937.6 = 2696$
Sources brighter than 10 mJy = 8
Total expected bright sources from VLASS = 8* 33885/2937.6 = 98

Figure 3 (a) and 3 (b) show flux density and spectral index distribution, respectively, for 50 sources obtained by cross-matching with the NVSS (section 2.1). Most of these sources fall around the spectral index between -0.5 and -1.0. Two of these sources have steep spectral index < -3. One of them is the above mentioned Seyfert galaxy. These galaxies have been excluded from spectral index histogram (Figure 3 (b)). As we observe a source at a higher frequency, it gets more resolved, the measured flux density reduces and hence, we see steeper spectra.

We compare spectral index with the known SMBBH candidates. The spectral index for C1 and C2 in 0402+379 are -0.8 and -0.46, and -0.33 and -0.38 for NGC7674. This further solidifies that such sources are most likely AGNs. It will be possible to obtain spectral values for all VLASS candidates once the survey is complete. Note that we do not use the spectral index as our source selection criteria for our census. We only use it to obtain additional information.

2.3 Error in source count

Quick-look images from VLASS may contain artifacts since they haven't been cleaned deeply enough, hence, it's likely to have a few false detections. The false detection rate depends on the signal to noise ratio of a source. For our catalog, we have used 7σ as the source selection criteria. Each tile covers about 1.33 hr in RA (Varies with the declination, ranges between 0.67 to 1.33) and 4 degrees in Declination. Using this, we estimate the probability of having a false detection in our sample as been discussed below.

Beam Area of an VLASS image $\sim 9e-04$ deg $\times 6e-04$ deg

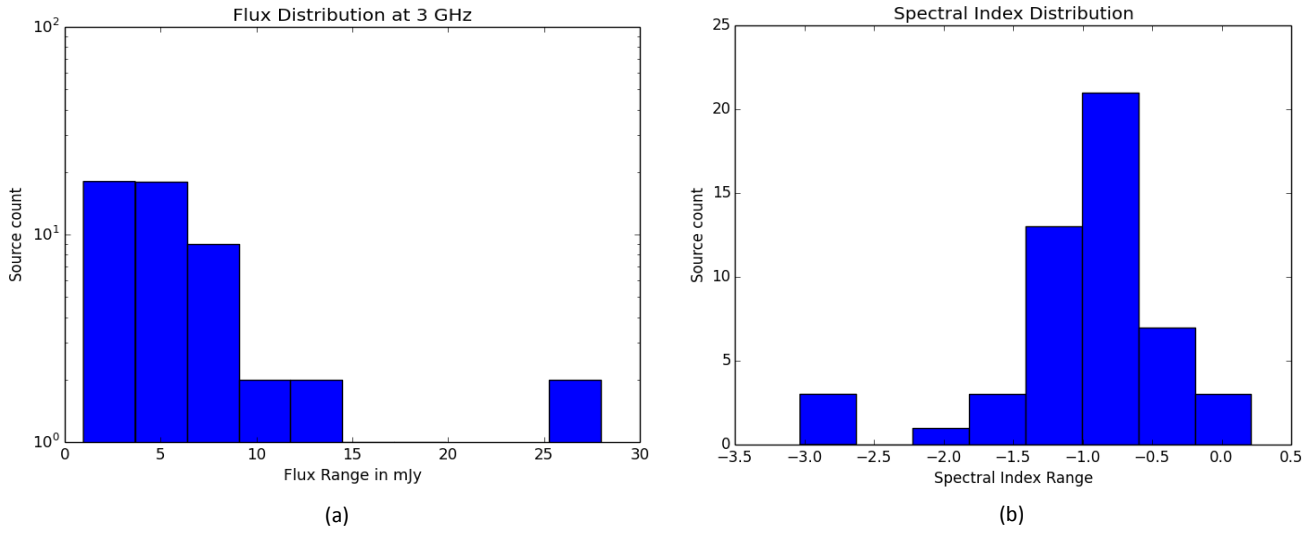

Figure 3: Flux distribution (a) and Spectral Index distribution (b) of 50 sources obtained from cross matching VLASS, SDSS, and NVSS (sec 3).

Total number of beams in our selected coordinates = $\frac{TotalArea}{BeamSize}$
Assuming each beam corresponds to a probable source on the map,
For 7σ, probability of finding a wrong detection = 2.55e-12
Number of false detections =Number of beams $\times$ probability = 0.01

As per the above calculation, the number of false detections is expected to be less than unity. This assumes no systematic errors such as RFI or side lobes from a bright source.

3 Proposed ngVLA Configuration

There are two major constraints on an instrument while conducting sky observations: resolution and sensitivity. The resolution of an array is determined by the longest baseline and the observing frequency. For studying SMBBHs and determining their orbital motion within $\sim$ 10 yrs, a resolution of the order of $\sim$ 0.1 mas is required to resolve the separation between compact cores. At the moment, this capability is only available with the VLBA, which offers the longest baseline of about 8000 km, while operating at frequencies ranging from $1 - 90$ GHz. ngVLA is expected to operate between $1.2 - 116$ GHz, which extends the high frequency limit. In Table 3, we list the expected angular resolution using ngVLA for three different maximum baselines 300 km, 1000 km, and 10000 km. We find that only large baselines comparable to 10,000 km will provide us the desired resolution to probe SMBBHs. It would be impossible to study SMBBHs without them. In order to obtain the resolution equivalent to VLBA, we suggest replacing existing VLBA antennas with the ngVLA antennas. These new antennas will also enhance the performance since they will be based on new technology.

Now the question arises how many antennas should replace the pre-existing VLBA antennas. Area of each VLBA antenna is 491 m^2, which is twice the surface area of each ngVLA dish with a diameter of 18 m. Image sensitivity of an instrument is given by the following equation in units of Jy beam^{-1}:

$$\sigma_{NA} = SEFD^* / \sqrt{(2\ \eta^2 N_{pol}\, \delta\nu\ t.} \tag{2}$$

where,

$$SEFD^* = \frac{1}{\sqrt{\Sigma_{i,j}^{N_{ant}, i<j} \frac{1}{SEFD_i * SEFD_j}}}, \tag{3}$$

and,

$$SEFD_i = 2k_B T_{sys}/(\eta_Q \eta_A A_i) \tag{4}$$

On comparing the SEFD of ngVLA antennas with that of VLBA across all the frequencies in Table 3, we note that they don't differ much within the frequency range $8 - 43$ GHz, and is roughly three times less at 93 GHz. ngVLA with a larger number of baselines as well as the bandwidth (Table 3) compared to VLBA, will contribute to the overall sensitivity.

For our study, we need better sensitivity on long baselines. SEFD for ngVLA and VLBA have been obtained from Memo 17 (2017) and Observational Status Summary (OSS [2]) for VLBA, respectively. We estimate image sensitivity (RMS) for different ngVLA configurations such that the number of ngVLA antennas replacing each VLBA antenna varies. This would lower the SEFD as it depends on the area of an antenna (equation 4) and will also reduce the overall image RMS. If we increase the number of antennas at each VLBA station by n, SEFD of that station will go down by a factor of n. Note that SEFD will be affected only at VLBA stations, and will remain the same for rest of the antennas. For RMS calculation, we consider the long baselines (similar to VLBA, 45), as small baselines will not contribute to image sensitivity at our resolution. We also include the core of the ngVLA array which consists of a phased array of 94 antennas (Memo 47, 2018). This would provide 10 additional baselines. It is assumed that baseline sensitivity will be sufficient for fringe fitting.

In this study, we predict about 2700 SMBBH candidates in the complete VLASS, of which about 100 candidates have flux density > 10 mJy at 3 GHz. Note that all the above measured flux densities may include flux from the radio jets in the galaxy which implies weaker core components and demands higher sensitivity. As the frequency of observation goes towards the higher end of the spectra, the source starts to resolve more. Hence, the flux of the core reduces which requires a more sensitive instrument. SEFD of VLBA antennas at higher frequencies is much larger in comparison to low frequencies. Thus, in order to conduct multi-frequency studies, better sensitivity is required at higher frequencies. Multi-frequency studies are essential to correct for core-shifts Sokolovsky et al. (2011) as in 0402+379 (Bansal et al., 2017). As a side benefit, they allow us to measure magnetic fields near the black hole.

We estimate expected flux density across all frequencies for one test candidate with flux density equal to 1 mJy at 3 GHz, weakest in our sample, assuming a spectral index of -0.75 (Figure 3). The current sensitivity of the VLBA station for 10 minutes of observation at 24 GHz (Table 3) with the current configuration is 0.07 mJy beam^{-1}. In order to observe this SMBBH candidate (Table 3) using the ngVLA with a signal to noise (SNR) of ~ 100, we need almost 35 times better sensitivity than that of VLBA at this frequency. Higher SNR helps us constrain the positions better which in turn will help us constrain the motion parameters.

It is obvious as we increase the number of antennas at each station, the sensitivity also increases. So in order to constrain this number, we have estimated five RMS values, denoted as RMS $1 - 5$ for 10 min long observations, listed in Table 3. These RMS values have been obtained using equation 2 and 3 for different number of ngVLA antennas at each VLBA station combined with the core (phased array of 94 antennas) of the array. The overall image RMS decreases with antenna count. ngVLA with three antenna substitution will have SNR of ~ 276 at 8 GHz, ~ 166 at 17, ~ 97 time at 28 GHz, ~ 54 at 41, ~ 12 at 93 GHz. This configuration with three ngVLA antenna at each VLBA site, suffices our sensitivity criteria so we would not require additional antennas. The main reason for this improvement aside from the large collecting area, is the increased bandwidth of ngVLA and inclusion of core. (Table 3).

[2]https://science.nrao.edu/facilities/vlba/docs/manuals/oss/bands-perf

Table 3: Observational parameters comparison

		ν (GHz)				
Source	Parameters	8	17[a]	28[b]	41	93[c]
ngVLA	Resolution for B_{max} = 300km (mas)	26	12	7	5	2
	Resolution for $B_{max} = 1e3$km (mas)	7.7	3.6	2.2	1.5	.70
	Resolution for $B_{max} = 1e4$ km (mas)	0.77	0.36	0.22	0.15	0.07
VLBA	SEFD(Jy)	327	543	534	1181	4286
	RMS (mJy beam^{-1})	0.04	0.07	0.07	0.16	0.73
ngVLA	SEFD (Jy)	324.8	302.0	457.7	738.2	1817.5
	RMS 1 (mJy beam^{-1})	0.0031	0.0030	0.0035	0.0047	0.0116
	RMS 2 (mJy beam^{-1})	0.0022	0.0021	0.0024	0.0033	0.0080
	RMS 3 (mJy beam^{-1})	0.0017	0.0016	0.0019	0.0026	0.0064
	RMS 4 (mJy beam^{-1})	0.0015	0.0014	0.0016	0.0022	0.0054
	RMS 5 (mJy beam^{-1})	0.0013	0.0012	0.0014	0.0019	0.0048
	BW (GHz)	8.7	8.4	14	20	20
Test Source	S_ν (mJy beam^{-1})	0.48	0.27	0.19	0.14	0.08
0402+379	S_ν (mJy beam^{-1}) C1	83	50	36	28	16
	S_ν (mJy beam^{-1}) C2	18	13	11	9	7
NGC 7674	S_ν (mJy beam^{-1}) C1	–	0.71	0.60	0.53	0.41
	S_ν (mJy beam^{-1}) C2	–	0.72	0.61	0.54	0.40

[a,b,c]VLBA frequencies are 15, 24, and 86 GHz

Notes: Resolution for ngVLA at three maximum baselines. RMS values for both VLBA and ngVLA have been estimated for 10 min long observation using equation 2. RMS 1 to RMS 5 differ in number of ngVLA antenna in place of one VLBA antenna with one to five antennas combined with the core (Memo 47, 2018), respectively. Bandwidth of VLBA is 512 MHz per polarization. For 0402+379 and NGC 7674, flux densities at higher frequencies have been estimated using the spectral index values listed in Bansal et al. (2017) and Kharb et al. (2017), respectively.

This suggests that we need to replace current VLBA antennas with 3 ngVLA antennas and conduct observations in frequencies ranging from 8−41 GHz to obtain the required sensitivity and frequency coverage. In order to study 2700 SMBBH candidates with the ngVLA, it would require an observation time of at least 27000 minutes $\sim$ 450 hours, with 10 min observation time on each source.

4 Conclusion

We obtain a census of SMBBH candidates using the VLASS survey and obtain 221 sources after cross matching them with the SDSS. These sources are nearby and bright. For 50 of those sources, we are able to obtain the spectral index using the 1.4 GHz flux density from NVSS. The spectral index values are mostly between -0.5 and -1.0 which includes a confirmed source: 0402+379 and a known SMBBH candidate: NGC 7674. This additional information is useful in improving the confidence level of our sample.

We predict 2700 SMBBH candidates once the VLASS is complete. In order to study these sources in more detail, we explore plausible baselines as well as frequencies for ngVLA to obtain the desired resolution and sensitivity. Radio sources emitting via synchrotron

emission have low flux density at higher frequencies, whereas, higher frequencies provide better resolution. This illustrates a tension between sensitivity and resolution. We find that an ideal array for our study would replace the VLBA antenna with a cluster of 3 ngVLA antenna at each station. It is important to note that in spite of a large number of antennas in ngVLA, only long baselines will enable this study, however, the core of the array improves the sensitivity. ngVLA with multi-frequency observations will also enable us to study the core shift effect which provides a measure of magnetic field near the core. For this purpose, frequencies ranging between 8−41 GHz will be suitable. This shows how ngVLA will be essential in observing SMBBH candidates including the relatively weak sources.

References

Blanton, M. R. and Bershady, M. A. and Abolfathi, B. and Albareti, F. D. et al. 2017, arXiv:1703.00052

Bansal, K., Taylor, G. B., Peck, A. B., Zavala, R. T., & Romani, R. W. 2017, ApJ, 843, 14

Begelman, M. C., Blandford, R. D., & Rees, M. J. 1980, Nature, 287, 307

Burke-Spolaor, S. 2011, MNRAS, 410, 2113

Comerford, J. M., Gerke, B. F., Stern, D., et al. 2012, ApJ, 753, 42

Condon, J. J., Cotton, W. D., Greisen, E. W., Yin, Q. F., Perley, R. A., Taylor, G. B., & Broderick, J. J. 1998, AJ, 115, 1693

Cuadra, J. and Armitage, P. J. and Alexander, R. D. and Begelman, M. C., MNRAS, 2009, 393,1423

Gunn, J.E. and Siegmund, W.A. and Mannery, E. J. and Owen, R.E. and Hull et al. 2006, ApJ, 131, 2332

Khan, F.M. and Just, A. and Merritt, D., ApJ, 2011, 732, 89

Kharb, P., Vir Lal, D., & Merritt, D. 2017, arXiv:1709.06258

Klein, A., Barausse, E., Sesana, A., et al., 2016, PhysRevD, 93, 024003

McConnell, N. J. and Ma, C.-P. and Gebhardt, K. et al., Nature, 2011, Dec, 480, 215

R. Selina, E. murphy ngVLA Memo 17, 2017

C. L. Carilli ngVLA Memo 47, 2018

Mohan, N. & Rafferty, D. 2015, arXiv:1502.007

Milosavljević, M., & Merritt, D. 2003, ApJ, 596, 860

Roedig, C. and Sesana, A. and Dotti, M. et al., 2012, A&A, 545, A127

Sokolovsky, K. V., Kovalev, Y. Y., Pushkarev, A. B. et al. 2011, A&A, 532, A38

Tremblay, S. E., Taylor, G. B., Ortiz, A. A., et al. 2016, MNRAS, 459, 820

Amy Kimball, VLASS Project Memo 7, 2017